THE JOURNAL OF PHYSICAL CHEMISTRY A

Article

pubs.acs.org/JPCA

Preferred Configurations of Peptide−Peptide Interactions

Upendra Adhikari and Steve Scheiner*

Department of Chemistry and Biochemistry, Utah State University, Logan, Utah 84322-0300, United States

Supporting Information

ABSTRACT: The natural and fundamental proclivities of interaction between a pair of peptide units are examined using high-level ab initio calculations. The NH···O H-bonded structure is found to be the most stable configuration of the *N*-methylacetamide (NMA) model dimer, but only slightly more so than a stacked arrangement. The H-bonded geometry is destabilized by only a small amount if the NH group is lifted out of the plane of the proton-accepting amide. This out-of-plane motion is facilitated by a stabilizing charge transfer from the CO π bond to the NH σ^* antibonding orbital. The parallel and antiparallel stacked dimers are nearly equal in energy, both only slightly less stable than the NH···O H-bonded structure. Both are stabilized by a combination of CH···O H-bonding and a $\pi \rightarrow \pi^*$ transfer between the two CO bonds. There are no minima on the surface that are associated with $O_{lp} \rightarrow \pi^*(CO)$ transfers, due in large part to strong electrostatic repulsion between the two O atoms, which resists an approach of a carbonyl O from above the C═O bond of the other amide.

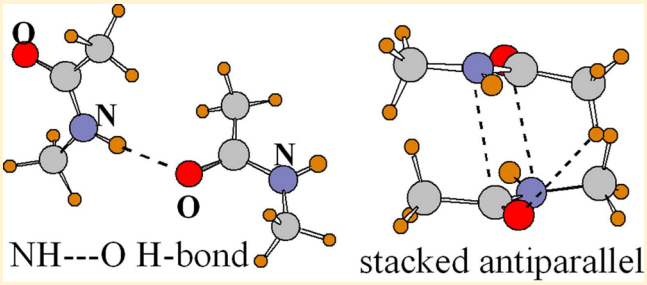

INTRODUCTION

Amidst a broad range of phenomena in which H-bonding plays a prominent role, perhaps none are so important as the H-bonds occurring in proteins. These noncovalent bonds are one of the prime ingredients in protein structure and function. They are widely accepted to be largely responsible for such prevalent secondary structures as α-helices and β-sheets, wherein pairs of peptide units engage in stabilizing NH···O═C H-bonds. Their influence is exerted also in other less common structural units within proteins, some particular to a given molecule.

While there is widespread agreement concerning the value of these interpeptide H-bonds, there remain some lingering but important questions as to the relative geometries that a pair of peptide units would prefer to approach one another. It is commonly thought, for example, that the θ(NH···O) angle tends toward linearity as is the case with other H-bonds. Yet even that being the case, does the NH favor an approach along the C═O axis, or would it be preferable for the NH to lie along one of the two carbonyl "rabbit ear" lone pairs? The latter idea implies that the NH ought to lie in the plane of the proton-accepting peptide unit. However, there are a host of crystal structure surveys that suggest that placement of the NH out of this plane is quite a common occurrence, more frequent than would be explained simply by other forces of the protein pulling the NH out of the plane against its wishes.

In addition to the presumed NH··O H-bonds, there have been several other mechanisms of attraction that have found support in the literature. The notion of attractive interactions between simple carbonyl groups derives from crystal structure analyses[1,2] which point toward parallel, antiparallel, and perpendicular arrangements, and were attributed to simple dipolar interactions.[3] Calculations[4] of pairs of esters pointed toward charge transfer from the lone pair of one O to the π^* antibond of the other. A perpendicular arrangement of carbonyl groups was tested via model systems[5] where it was found to be stabilizing albeit only weakly, comparable to a CH··π H-bond. However, the calculations assumed a particular orientation and did not test to determine whether or not this was a true minimum in the surface.

Recent work by the Raines group[6−9] has made a case that $n \rightarrow \pi^*$ electron transfer from a carbonyl O lone pair to the π^*(CO) antibonding orbital of the partner peptide can exert a strong influence, particularly in helical structures and β-sheets,[10] and one that is stronger in true peptide−peptide interactions than in many peptidomimics.[11] It is proposed that this force enables a surprisingly close approach of the O atoms of the two peptide groups, and bypasses the idea of a NH···O H-bond. Another work[12] found orthogonal C═O···C═O interactions to be "a substantial intermolecular association force capable of inducing self-assembly in apolar, non-competing solvents".

A second, and more recent, concept that underlies interpeptide attraction arises from studies of small oligopeptides in the gas phase.[13−16] In some of the conformations observed, pairs of peptide units arrange themselves parallel to one another, in a stacked geometry. In addition to an electrostatic attraction that might arise from the antiparallel arrangement, a charge transfer to a CO π^* antibonding orbital is suggested here. Yet unlike the aforementioned carbonyl−carbonyl attraction, in this case the source of the density is the

Received: November 5, 2012
Revised: December 23, 2012
Published: December 28, 2012

N lone pair. Zwier et al. suggest[14] that this stacking motif might not be limited to small di- and tripeptides but may well contribute to the folding of the much larger proteins. There was some precedent for this parallel arrangement derived from studies of pairs of carboxyl groups[17] where again a parallel arrangement was observed. The authors explained the attraction by a combination of dipole−dipole and of n→π^* charge transfer.

These ideas lead to the obvious question as to what exactly are the preferred arrangements of peptide groups. Is a coplanar pair with a linear NH··O H-bond truly energetically superior to the approach of the NH from above the plane of the partner peptide? Is a H-bonded structure indeed preferred, as is commonly supposed, to the approach of the two carbonyl groups toward one another? Also, how does a stacked arrangement fit into the broader picture; are there occasions in which such a geometry might actually be superior? These are issues that can be addressed in a straightforward manner by quantum chemical calculations.

Also, as one might expect, the importance of the peptide−peptide interaction has motivated a good deal of prior theoretical scrutiny.[18−24] Because of the delicacy involved in comparisons of different sorts of geometries, with differing origins of stability, it would be injudicious to base any decisions of relative stability on any but high-level correlated calculations, of which there have been several performed in recent years. Concerning studies of peptide analogues such as formamide and *N*-methylacetamide, the majority were limited primarily to standard H-bonded geometries,[25−29] especially those wherein the two molecules occupied the same plane.[30−34] There have been a handful of works that went beyond this simple paradigm and noted dimer geometries that had significant elements of nonplanarity,[35−39] but did not pursue this issue in any detail. Others considered only specific orientations that occur in protein secondary structures such as α-helix and β-sheet[40] without determining whether or not they correspond to minima on the potential energy surface, nor making comparisons to such minima. Although receiving only scant attention, stacked arrangements have not been entirely ignored. Vargas et al.,[41] for example, considered stacked pairs of dimethylformamide, but their analysis of the origin of the stability of this structure was superficial. The authors did not consider electrostatic or charge transfer effects explicitly, rationalizing the geometry purely on the basis of purported CH··O H-bonds, despite their highly distorted nature, leaving in question their categorization as H-bonds.

The present work comprises a comprehensive examination of the various attractive interactions that may occur between a pair of peptide groups. The *N*-methylacetamide (NMA) molecule, $CH_3NHCOCH_3$, is taken as a model of the peptide unit, as the amide group is surrounded on both sides by the C atom that occurs within the context of a protein. The trans geometry of NMA was considered, again due to its similarity to the protein backbone. The potential energy surface of the NMA dimer is thoroughly probed so as to identify all minima, with no preconceived notions as to what these ought to be. The source of stability of each minimum is analyzed by various means including identification of any significant charge transfers, decomposition of the interaction energy into its various components, and interaction between electrostatic potentials of the two subunits. Most importantly, the application of high-level ab initio calculations facilitates a quantitative comparison of the relative energies of all minima on the surface to establish the fundamental preferences of peptide−peptide interactions.

COMPUTATIONAL METHODS

Calculations were carried out via the Gaussian 09 package.[42] All geometries were optimized at the ab initio MP2/aug-cc-pVDZ level of theory, which has been shown to be of high accuracy especially for those systems with intermolecular interactions of the type of interest here[43−49] where the data are in close agreement with CCSD(T) with larger basis sets.[50−52] Optimizations were carried out both with and without inclusion of counterpoise[53] in the algorithm. The potential energy surface of the NMA dimer was examined thoroughly to identify all possible minima by optimizing from a range of possible starting points. Minima were verified as having all positive vibrational frequencies. Binding energies were evaluated as the difference between the energy of the dimer and twice that of the fully optimized NMA monomer, with counterpoise correction of basis set superposition error. Natural bond orbital (NBO)[54,55] analyses were carried out via the procedure contained in Gaussian. The binding energy was decomposed by symmetry adapted perturbation theory[56] (SAPT) using the Molpro[57] set of codes.

RESULTS

All minima obtained when counterpoise is included directly in the optimization algorithm are displayed in Figure 1. Structures

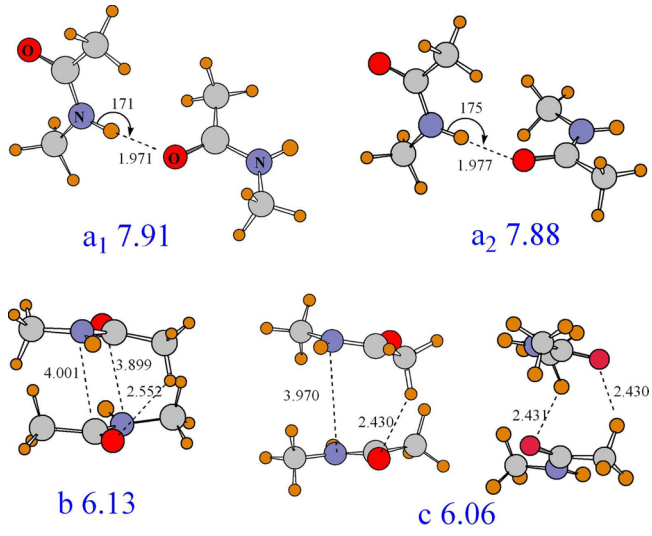

Figure 1. Geometrical dispositions of two NMA molecules in fully optimized dimers, with counterpoise corrections included in the optimization algorithm. Binding energies reported as large blue numbers; distances in Å and angles in degrees. Two views are presented of dimer **c** so as to view both CH··O H-bonds.

$\mathbf{a}_1$ and $\mathbf{a}_2$ may be categorized as containing standard NH···O H-bonds. They are very similar to one another, differing primarily in a rotation of the righthand NMA molecule around its C═O axis. Consequently, the binding energies, both nearly 8 kcal/mol, are almost identical to one another, as indicated by the large blue numbers in Figure 1. The θ(NH··O) angle is within 9° of linearity in both, reported in Table 1, as expected for a H-bond, and the R(H···O) H-bond lengths are less than 2 Å. The θ(CO··H) angles differ a bit, 120° for structure $\mathbf{a}_1$ and 142° for $\mathbf{a}_2$. This deviation from linearity is consistent with the idea of a

dx.doi.org/10.1021/jp310942u | J. Phys. Chem. A 2013, 117, 489−496

Table 1. Geometric and Energetic (kcal/mol) Aspects of NH··O H-Bonded Dimers

	$\mathbf{a}_1$	$\mathbf{a}_2$
ΔE	7.91	7.88
R(H···O), Å	1.971	1.977
θ(NH···O), deg	171	175
θ(CO···H), deg	120	142
φ(H··OCN), deg	−171	−6
φ(CN··OC), deg	−76	−77
$E(2)$ $O_{lp}\rightarrow\sigma^*$NH	13.82	12.56

pair of roughly equivalent "rabbit ear" lone pairs on the carbonyl O. Also, consistent with this notion, the bridging proton lies very close to the amide plane of the proton-acceptor molecule, with φ(H··OCN) dihedral angles within 6−9° of a fully planar arrangement. The amide planes of the two molecules are close to perpendicular, with φ(CN··OC) dihedral angles of nearly 80°. The last row of Table 1 shows a strong NBO second-order perturbation energy that corresponds to charge transfer from the O lone pairs to the NH σ^* antibonding orbital, a well-understood aspect of a standard H-bond of this sort.

Structures **b** and **c** in Figure 1 are roughly similar to one another, in that both have the two amide planes stacked above one another. They differ primarily in their relative orientations: **b** can be described as antiparallel in that the NH of one amide lies above the C═O of the other. **c** represents a parallel structure with the two NH groups stacked above one another as are the pair of C═O groups. Note however that the two NH groups point in opposite directions, as do the two C═O groups. As another important point, the stacking is not perfect in the sense that the two amide planes are not fully parallel to one another in either **b** or **c**. The tilt allows a methyl group of the upper amide to engage in a CH··O H-bond with the lower carbonyl in **b**; there are two such CH···O H-bonds in **c**.

NBO analysis of these structures provides a mechanism to understand the individual elements of the binding. Both **b** and **c** include transfer from the π bond of one carbonyl to the π^* antibond of the partner C═O, and vice versa. This transfer is confirmed by examination of the populations of the relevant NBOs. Formation of stacked complex **b**, for example, reduces the CO π-orbital population by 2−3 me relative to the monomer, whereas the π^* MOs gain between 2 and 7 me. The $E(2)$ $\pi\rightarrow\pi^*$ energetic contribution is twice as large in **b** as in **c**, 1.36 vs 0.68 kcal/mol, as reported in Table 2. Both structures also include CH··O H-bonding, but there is more of it in **c**. More precisely, the two CH··O H-bonds in **c** add up to $O_{lp}\rightarrow\sigma^*$(CH) $E(2)$ of 2.26 kcal/mol, versus only 0.78 for the single CH··O H-bond of **b**. Also, all three of these H-bonds are supplemented by a very significant element of charge transfer to the σ^*(CH) from the CO π bonding orbital, 1.56 and 0.39 kcal/mol for **c** and **b**, respectively. The NBO data suggest then that both stacked structures contain elements of both $\pi\rightarrow\pi^*$ transfer and CH··O H-bonding. The former is more important in antiparallel structure **b** and the latter plays a larger role in **c**, partly because there are two such CH··O H-bonds here. The interatomic distances support this distinction. The C···C distance in **b** is some 0.05 Å shorter in **b** than in **c**, and the H-bonds in **c** shorter by 0.12 Å.

Table 2. Geometric and Energetic (kcal/mol) Aspects of Stacked Dimers

	b	**c**
ΔE	6.13	6.06
R(C···C), Å	3.370	3.425
$E(2)$ π(CO)$\rightarrow\pi^*$(CO)	1.36	0.68
R(H···O), Å	2.552	2.430
$E(2)$ $O_{lp}\rightarrow\sigma^*$(CH)	0.78	2.26
R(H···C), Å	3.298	3.122
$E(2)$ π(CO)$\rightarrow\sigma^*$(CH)	0.39	1.56

The decomposition of the total interaction energy into its constituent parts can aid in the analysis of the underlying differences between the minima. The components of SAPT deconstruction[56] are reported in Table 3 for the four structures of Figure 1. There are certain similarities among all four. For example, in all cases, the electrostatic term is the largest attractive component, followed by dispersion, and then by induction. Yet a closer examination reveals some substantive differences. In the first place, the electrostatic energy is considerably larger in the structures containing standard NH···O H-bonds as compared to the stacked dimers. This pattern reverses in the case of dispersion, which is larger in the two latter geometries. In terms of patterns, the induction energy is almost as negative as dispersion in these NH··O structures, whereas the latter is 2−3 times larger than the former for the stacked geometries. In fact, the dispersion energy is very nearly as large as the electrostatic attraction in the stacked structures. In summary, the comparison of stacked to NH··O structures indicates a reduced electrostatic term and increased dispersion energy.

Table 3. SAPT Contributions (kcal/mol) to Total Interaction Energies of NMA Dimers

	NH···O		stacked	
	$\mathbf{a}_1$	$\mathbf{a}_2$	**b**	**c**
ES	−11.25	−10.46	−8.02	−7.41
EX	9.39	8.51	7.20	7.32
IND	−4.23	−3.69	−3.44	−2.87
IND+EXIND	−2.10	−1.97	−1.38	−1.34
DISP	−5.33	−5.38	−7.01	−6.82
DISP+EXDISP	−4.54	−4.66	−6.13	−6.00
total	−8.50	−8.58	−8.33	−7.44

One may glean some insight into the origin of the electrostatic attraction by examination of the electrostatic potentials of each pair of monomers. These potentials are superimposed on the positions of the monomers within the context of each optimized dimer in Figure 2 where the blue contours represent positive regions, and negative is signified by red. The potential around the NMA monomer is largely positive in most areas, but contains a very prominent negative region that surrounds the carbonyl O atom. In all three cases, whether the NH··O H-bonded dimer $\mathbf{a}_1$, or the stacked geometries, the negative red region of one molecule approaches a blue positive area of the partner molecule. In both **b** and **c**, the O atoms of both molecules participate in this electrostatic attraction. The more attractive electrostatic component for the H-bonded structure $\mathbf{a}_1$ can be rationalized on the basis of the very direct interaction between positive and negative regions, as compared to the parallel arrangement in **b** and **c**. This comparison bears a certain resemblance to that between σ and π bonds.

dx.doi.org/10.1021/jp310942u | J. Phys. Chem. A 2013, 117, 489−496

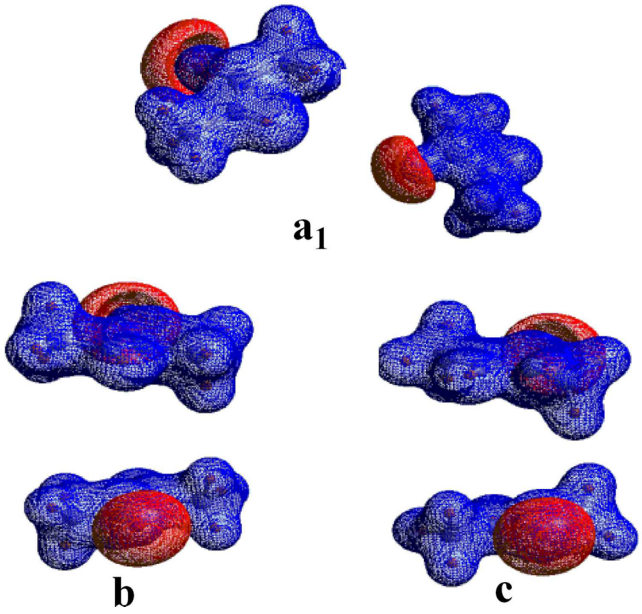

Figure 2. Electrostatic potentials of two NMA subunits in each of three different dimers. Blue regions correspond to positive potential, negative to red. Contour illustrated is 0.08 au.

Another window into the nature of the interaction can be opened via examination of electron density shifts that accompany dimerization. Figure 3 illustrates the difference in

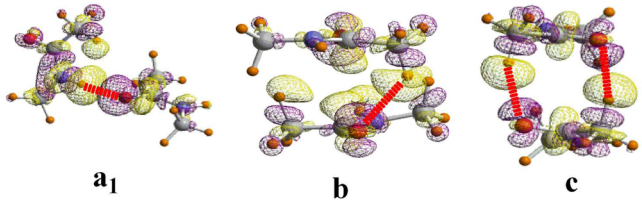

Figure 3. Shifts of electron density occurring in three NMA dimers. Purple regions denote added density, while losses are shown in yellow. Contour illustrated is 0.0008 au. H-bonds are indicated by a broken red line.

the density of each complex, with respect to the sum of the densities of the two monomers, in the same internal geometries and positions that they adopt in the complex. Increases in density, indicated by purple regions, correspond to shifts of density into that area upon complexation; yellow areas denote decreases. The most substantial shift in complex $\mathbf{a}_1$ occurs right along the NH··O H-bond, indicated by the broken red line. The pattern of charge shift away from the bridging proton and into the purple regions on either side of it is characteristic of a H-bond. This same pattern is noted in the CH···O H-bonds of **b** and **c**, further bolstering the contention that these dimers are held together in part by such H-bonds.

As indicated above, the two stacked dimers are attracted to one another in part by transfer from the CO π orbital of one molecule to CO π^* of the partner, with a symmetric transfer occurring in the opposite direction. It is thus no surprise to note large shifts above and below each monomer, with very little taking place within each molecular plane of **b** and **c**. In other words, one can speak of large π shifts and very small σ shifts. There is a shift of density toward the O atoms, both above and below the molecular plane. Yet this increase is notably larger in the region between the two molecules. Likewise, there is a loss of density above and below the C atoms, albeit slightly smaller in magnitude than those associated with O; little change is observed near the N atoms. This pattern is what one might anticipate if the two monomers engage in π(CO)→π^*(CO) charge transfers, as suggested by Table 2. Note also that the shifts above and below the carbonyl planes are more substantial in **b** than in **c**, again consistent with the more prominent role played by π→π^* transfers in **b**.

Sensitivity to Basis Set Superposition Error. In most cases in the literature, counterpoise corrections are added to a structure that has been optimized on an uncorrected surface.[58,59] An alternate procedure, albeit a somewhat more time-consuming one, performs the geometry optimization on a fully corrected potential energy surface. As such, it is normally found that the intermolecular distance is somewhat longer in the latter case, as the artificial attraction associated with basis set superposition error does not pull the two subunits too close together. Yet other than this small change in intermolecular separation, the minima optimized on the corrected and uncorrected surfaces are typically quite similar.

The NMA dimer represents a departure from this general observation. Significant differences in optimized geometry were noted first in the NH··O H-bonded complexes. The φ(H··OCN) angles listed in Table 1 for $\mathbf{a}_1$ and $\mathbf{a}_2$ are −171° and −6°, respectively, both rather close to the placement of the bridging proton in the plane of the proton-accepting NMA molecule. In contrast, when the optimizations were performed without including counterpoise corrections at each step, the NH proton was positioned quite a bit out of this plane. Details of these structures are provided in Table 4, where it may be seen from the φ(H··OCN) dihedral angles that the proton in question hovers between 50° and 65° above the plane of the partner amide. Because of this departure from the plane, the proton is further removed from the acceptor carbonyl O than in the planar cases of Table 1, despite the artificial attraction that arises from the basis set superposition error. Also, one might also note the greater disparity from H-bond linearity in these nonplanar structures, with θ(NH··O) between 137° and 155°, as compared to 171°−175° for the planar complexes. (The four structures described in Table 4 are quite similar to one another,

Table 4. Geometric and Energetic Aspects of NH··O Dimers Obtained without Inclusion of Counterpoise Corrections in Optimization Algorithm

ΔE,[a] kcal/mol	r(H··O), Å	θ(NH··O), deg	φ(H··OCN), deg	O_{lp}→σ^*NH $E(2)$, kcal/mol	r(H··C), Å	π(CO)→σ^*NH $E(2)$, kcal/mol
7.28	1.985	155	−56	7.95	2.759	3.01
7.01	2.030	149	130	6.84	2.667	2.57
6.90	1.999	148	65	5.85	2.606	4.24
6.47	2.088	137	116	4.02	2.671	2.80

[a]Including counterpoise correction after optimization.

dx.doi.org/10.1021/jp310942u | J. Phys. Chem. A 2013, 117, 489−496

differing primarily in the disposition of one molecule relative to another. Their geometries are displayed graphically in Figure S1 of the Supporting Information, along with all other minima obtained on the uncorrected potential energy surface.)

One consequence of the displacement of the NH from the carbonyl plane is a perturbation in the NBO E(2) quantity that reflects the transfer from the O lone pairs to the NH σ^* antibond. As compared to values between 12.6 and 13.8 kcal/mol in the planar geometries, this quantity drops to between 4 and 8 kcal/mol when the H is situated above the plane of these O lone pairs. In partial compensation, a new charge transfer appears, one in which the density is removed from the CO π bonding orbital. $E(2)$ for this $\pi(CO)\rightarrow\sigma^*NH$ transfer amounts to between 2.6 and 4.2 kcal/mol, as reported in the last column of Table 4.

One may conclude from the distinctions between the H-bonded structures obtained on the corrected and uncorrected potential energy surfaces that a displacement of the NH out of the amide plane of the partner molecule is not energetically costly. Indeed, it requires scrupulous correction of superposition error to place these proton donors very close to the carbonyl plane. While disturbing the charge transfer from the O lone pairs to the NH σ^* antibond, nonplanarity permits transfer from the CO π bond to take its place to a certain degree.

Failure to include counterpoise corrections in the potential energy surface also has certain consequences for the stacked structures **b** and **c**. The largest perturbation arises in the antiparallel dimer **b**, designated **b′** in Figure S1. Instead of the tilt between the two molecules in **b** that leads to a CH··O H-bond, the two molecules lie precisely parallel to one another, with both **R**(N··C) distances equal to 3.710 Å. Without this tilt, the shortest intermolecular CH···O contact is 2.78 Å, beyond the range of a substantive H-bond. Also, indeed, there is no significant $E(2)$ that would correspond to any such CH··O H-bond. NBO analysis confirms the absence of this sort of H-bond with no significant $O\rightarrow\sigma^*(CH)$ transfer. On the other hand, the fully stacked arrangement of **b′**, as well as the closer approach of the two molecules, enhances the $\pi\rightarrow\pi^*$ charge transfer, with a combined $E(2)$ of 2.48 kcal/mol, as compared to the 1.36 kcal/mol in structure **b** where the molecules were tilted relative to one another. Structure **c′** is less distinct from **c**: The two molecules adopt essentially the same relative orientation in both. Also, in both cases, the R(C··C) distance is shorter than R(N··N) by about 0.5 Å, a tilt that facilitates formation of the two CH··O H-bonds. The latter are both 2.372 Å in length in **c′**, slightly shorter than the 2.430 Å in **c**, an expected result of failure to correct the surface for basis set superposition error.

As a consequence of including the counterpoise corrections into the optimization procedure, the final structures in Figure 1 are significantly more stable than those in Figure S1. For example, dimer $\mathbf{a}_1$ is more stable by 0.63 kcal/mol than the most stable configuration in Figure S1 where counterpoise is corrected after the fact. **b** and **c** are both more stable than **b′** and **c′** by 0.35 kcal/mol. In these cases, then, including counterpoise correction into the optimization affects not only the geometrical dispositions, but also the energies to a significant degree.

Influence of C═O Dipole−Dipole Attractions. The literature contains a number of instances in which a pair of carbonyl C═O groups approach one another in what might appear to be an attractive interaction.[3] Their mutual orientation can be either parallel or perpendicular.[1,2,17] Any such attraction has been attributed by some to simple dipole−dipole forces[1,3,5,12] whereby the negatively charged O approaches the C of the other carbonyl, which is of opposite charge. Another scenario considers $n\rightarrow\pi^*$ charge transfer from the O lone pairs to the carbonyl antibonding orbital of the other subunit.[4,6,10,11,17] With specific regard to amide units, recent studies of di- and tripeptides in the gas phase have found occasions where a pair of peptide units are stacked above one another,[13−15] as opposed to forming the normally expected NH···O H-bonds.

There are two minima, **b** and **c**, found by our calculations that can be described as stacked in some sense. They can be categorized as antiparallel and parallel, with binding energies of just over 6 kcal/mol, within about 2 kcal/mol of the preferred NH··O H-bonded structure. Although stacked, it cannot be said that the binding of either is attributable purely to $\pi\rightarrow\pi^*$ charge transfer, as both contain an essential element of CH···O H-bonding, more so for **c** than for **b**. At the same time, a fully parallel arrangement **b′**, with no significant H-bonding (see Figure S1), represents a stable minimum on the potential energy surface, albeit the surface without counterpoise corrections. Also, the binding energy of this dimer is only slightly less than that in **b** and **c**. So one might conclude that there is a strong theoretical basis for stacked arrangements of peptide units, whether fully parallel or tilted. Yet these structures do not show any evidence of the $n\rightarrow\pi^*$ charge transfers that have been hypothesized.

As there are no true minima in the NMA dimer surface that rely on the proposed $n\rightarrow\pi^*$ transfer as the basis of their stability, partial geometry optimizations were carried out with some restriction to search for such a structure. The O atom of one NMA molecule was placed directly above the C of the other, and the θ(O··CO) angle was held fixed at 90°. Such a prescription would allow the upper carbonyl to orient itself either perpendicular to the C═O below, or parallel to it. The optimization under this perpendicular sort of restriction led instead to an intermediate position, with θ(C···OC) = 135°, and R(C···O) = 2.805 Å. This orientation facilitates an interaction between a "rabbit ear" lone pair of the upper O and the C atom of the lower amide. In fact, a NBO perturbation energy $E(2)$ of 1.64 kcal/mol was evaluated for this $O_{lp}\rightarrow\pi^*(CO)$ charge transfer. This finding is consistent with the idea that such orientations can be stabilizing in peptide−peptide interactions, even if the geometry does not correspond to a true minimum on the NMA dimer surface. More quantitatively, the binding energy of this structure is only 1.71 kcal/mol, much smaller than those of the true minima, stabilized by NH··O or CH··O H-bonds and/or $\pi\rightarrow\pi^*$ charge transfer.

■ CONCLUSIONS AND DISCUSSION

The calculations have highlighted the minima on the potential energy surface of a pair of peptide units, each modeled by the NMA molecule. Two principal types of structure were found. The first class is stabilized by a classic NH···O H-bond, of the sort that is commonly considered to form between peptide units in such secondary structures as α-helices and β-sheets. The NH···O arrangement is very close to linear and the NH lies some 120−140° from the C═O axis, consonant with the idea of a pair of rabbit ear lone pairs on the O atom. The planes of the two amide groups are roughly perpendicular to one another.

There is a second type of dimer structure, which is slightly less stable, with a binding energy only 23% smaller. The two

dx.doi.org/10.1021/jp310942u | J. Phys. Chem. A 2013, 117, 489−496

amide units lie one above the other, in what may be termed a stacked configuration. The antiparallel structure places the CO of one molecule over the NH of the other, while the two CO groups lie directly above one another in the parallel arrangement, as do the two NH groups. There is only a very small energy difference between these two dimers. Part of the binding of these complexes arises from charge transfer from the CO π bonding orbital of one subunit to the antibonding π^*(CO) orbital of the other, and vice versa. A second stabilizing factor is one or more CH···O H-bonds. The former $\pi\rightarrow\pi^*$ transfer plays the dominant role in the antiparallel structure, while the CH··O H-bonds are more important in the parallel dimer. In contrast to an earlier work,[13] there was no evidence found here of a significant transfer to the CO π^* antibonding orbital from a N lone pair, even in the antiparallel stacked structure.

For all stable dimers, there is a strong electrostatic component to the attraction, as the negative potential surrounding the carbonyl O is situated in proximity to the positive potential of the partner molecule. This electrostatic attraction is somewhat larger for the NH··O H-bonded dimers. Induction and dispersion forces are substantial as well, albeit smaller than Coulombic attraction. Dispersion is a bit larger than induction, especially in the stacked dimers where dispersion is nearly as large as the electrostatic component.

One of the more interesting issues that arose in this study is the surprising degree of sensitivity of the equilibrium geometries to basis set superposition error. Failure to include counterpoise corrections within the optimization algorithm distorted the NH···O H-bonded configurations, lifting the bridging proton and NH group well out of the plane of the proton-accepting amide unit. The reason that this distortion did not strongly affect the binding energy is that the loss of some of the $O_{lp}\rightarrow\sigma^*$(NH) charge transfer is compensated by a new transfer into the NH σ^* antibonding orbital originating in the CO π bond. For example, the total $O_{lp}\rightarrow\sigma^*$(NH) $E(2)$ in dimer $\mathbf{a}_1$ is equal to 13.8 kcal/mol. This term is reduced to 8.0 kcal/mol in the distorted dimer where the NH is pulled out of the amide plane, but $E(2)$ for the π(CO)$\rightarrow\sigma^*$(NH) transfer of 3.0 kcal/mol makes up for some of this loss. One can thus conclude that the NH of one amide need not necessarily reside in the carbonyl plane, and that even large displacements out of this plane incur only a small energetic cost. This idea is reinforced by IR/UV double resonance data of a capped tripeptide chain in the gas phase[60] wherein the NH was located above the peptide plane of the CO proton acceptor.

A second perturbation in structure that is associated with basis set superposition error is the tilt angle between the two amide units in the stacked structures. While the parallel dimer is not affected much, the antiparallel conformation loses its tilt when this error is uncorrected, and the two molecules become perfectly stacked. Again, this change is facilitated by compensation. The loss of the CH···O H-bond in the tilted true minimum is offset by an increase in the $\pi\rightarrow\pi^*$ transfer between the CO bonding and antibonding orbitals. In quantitative terms of $E(2)$, the total in the true antiparallel, tilted minimum, arises from 1.4 kcal/mol for the $\pi\rightarrow\pi^*$ transfer plus 1.2 kcal from the CH··O H-bond. Although the latter is lost when the two molecules are fully stacked, the $\pi\rightarrow\pi^*$ $E(2)$ rises to 2.5 kcal/mol. This perturbation can be taken as an indication that the notion of stacked dimers needs not be taken too literally: some tilting is enabled by formation of CH···O H-bonds.

There is less evidence for the notion in the literature that there is a strong attraction between the carbonyl O of one group and the C atom of the other, in particular via a $O_{lp}\rightarrow\pi^*$(CO) charge transfer. There is no minimum on the surface that corresponds to such an interaction. When the two groups are placed accordingly, the structures quickly shift to one of the true minima in the surface. When the O atom is forced to lie directly above the carbonyl group, which would maximize an interaction of this type, there is some attraction noted, but it is rather weak, with only 22% of the binding strength of the NH···O structure, which represents the global minimum on the surface. One may conclude then that there is some validity to the idea of $O_{lp}\rightarrow\pi^*$(CO) stabilization, but this attraction is secondary to NH···O H-bonding structures, as well as the stacked arrangements that are stabilized by some combination of $\pi\rightarrow\pi^*$ and CH···O H-bonds.

NMA is of course only a model of the peptide unit in a full protein backbone. Nonetheless, it contains the essential elements of the peptide, which surrounds the amide group on both sides by a C atom that corresponds to the C^α of a protein. Also, it is the $C^\alpha H$ of the protein backbone that could participate in the CH···O H-bonds that represent a significant component in the stability of some of the stacked conformations. Yet it should be reiterated in this regard that such CH···O H-bonds are not crucial to these stacked configurations, as the loss of the latter H-bond can be compensated to a large degree by a more parallel arrangement of the amides, which adds to the $\pi\rightarrow\pi^*$ stabilization. Finally, there is little energetic distinction between the parallel and antiparallel arrangements of the two amide units. Both are beneficiaries of the Coulombic attraction between the negative potential surrounding the carbonyl O of one amide and the positive regions of the other portions of the second amide unit.

It is tempting to speculate how these results might be altered if the NMA molecules were enlarged to di-, tri-, or even larger oligopeptides. The first complicating issue would be the likely formation of internal H-bonds within each monomer. It is well-known, for example, that dipeptides tend to form C5 and C7 conformations that contain as an essential element NH···O H-bonds between adjacent peptide units.[61−63] The presence of any such internal H-bond could compete with NH···O H-bonds between amide units involving a separate partner molecule. On the other hand, the formation of an internal H-bond that occupies a NH group on one amide may not interfere with the ability of the C═O on the same peptide unit to act as proton acceptor to the NH of a neighboring molecule. Indeed, such an arrangement might be anticipated to strengthen the latter intermolecular H-bond, according to the principles of H-bond cooperativity, wherein proton donation from one part of a molecule tends to strengthen proton acceptance on a neighboring segment.[28,64,65] In fact, such positive cooperativity is a likely contributor to the stability of β-sheets containing three or more strands[23] or α-helices.[66,67] Not only conventional NH···O but also weaker CH··O are subject to comparable cooperativity effects[68−70] that might affect the stacked dimers in which they play some role. On the other hand, there is much less known about the positive or negative cooperativity that might arise in the stacking of multiple conjugated π systems, or concerning how the involvement in a H-bond might affect $\pi\rightarrow\pi^*$ charge transfers. For these reasons, an exploration of larger systems represents a ripe area for future research.

■ ASSOCIATED CONTENT

Supporting Information

Full refs 42 and 57 and Figure S1 illustrating geometries obtained without inclusion of counterpoise corrections in the optimization algorithm. This material is available free of charge via the Internet at http://pubs.acs.org.

■ AUTHOR INFORMATION

Corresponding Author

*E-mail: steve.scheiner@usu.edu.

Notes

The authors declare no competing financial interest.

■ ACKNOWLEDGMENTS

This work was supported by the National Science Foundation (CHE-1026826).

■ REFERENCES

(1) Allen, F. H.; Baalham, C. A.; Lommerse, J. P. M.; Raithby, P. R. *Acta Crystallogr.* **1998**, *B54*, 320−329.
(2) Santos-Contreras, R. J.; Martinez-Martinez, F. J.; Garcia-Baez, E. V.; Padilla-Martinez, I. I.; Peraza, A. L.; Hopfli, H. *Acta Crystallogr.* **2007**, *C63*, o239−o242.
(3) Paulini, R.; Müller, K.; Diederich, F. *Angew. Chem., Int. Ed.* **2005**, *44*, 1788−1805.
(4) DeRider, M. L.; Wilkens, S. J.; Waddell, M. J.; Bretscher, L. E.; Weinhold, F.; Raines, R. T.; Markley, J. L. *J. Am. Chem. Soc.* **2002**, *124*, 2497−2505.
(5) Fischer, F. R.; Wood, P. A.; Allen, F. H.; Diederich, F. *Proc. Natl. Acad. Sci. U.S.A.* **2008**, *105*, 17290−17294.
(6) Choudhary, A.; Gandla, D.; Krow, G. R.; Raines, R. T. *J. Am. Chem. Soc.* **2009**, *131*, 7244−7246.
(7) Kotch, F. W.; Guzei, I. A.; Raines, R. T. *J. Am. Chem. Soc.* **2008**, *130*, 2952−2953.
(8) Hodges, J. A.; Raines, R. T. *Org. Lett.* **2006**, *8*, 4695−4697.
(9) Hinderaker, M. P.; Raines, R. T. *Protein Sci.* **2003**, *12*, 1188−1194.
(10) Bartlett, G. J.; Choudhary, A.; Raines, R. T.; Woolfson, D. N. *Nat. Chem. Biol.* **2010**, *6*, 615−620.
(11) Jakobsche, C. E.; Choudhary, A.; Miller, S. J.; Raines, R. T. *J. Am. Chem. Soc.* **2010**, *132*, 6651−6653.
(12) Fäh, C.; Hardegger, L. A.; Ebert, M.-O.; Schweizer, W. B.; Diederich, F. *Chem. Commun.* **2010**, *46*, 67−69.
(13) James, W. H.; Buchanan, E. G.; Muller, C. W.; Dean, J. C.; Kosenkov, D.; Slipchenko, L. V.; Guo, L.; Reidenbach, A. G.; Gellman, S. H.; Zwier, T. S. *J. Phys. Chem. A* **2011**, *115*, 13783−13798.
(14) James, W. H.; Buchanan, E. G.; Guo, L.; Gellman, S. H.; Zwier, T. S. *J. Phys. Chem. A* **2011**, *115*, 11960−11970.
(15) James, W. H.; Muller, C. W.; Buchanan, E. G.; Nix, M. G. D.; Guo, L.; Roskop, L.; Gordon, M. S.; Slipchenko, L. V.; Gellman, S. H.; Zwier, T. S. *J. Am. Chem. Soc.* **2009**, *131*, 14243−14245.
(16) Buchanan, E. G.; James, W. H.; Choi, S. H.; Guo, L.; Gellman, S. H.; Müller, C. W.; Zwier, T. S. *J. Chem. Phys.* **2012**, *137*, 094301.
(17) Pal, T. K.; Sankararamakrishnan, R. *J. Phys. Chem. B* **2010**, *114*, 1038−1049.
(18) Scheiner, S.; Kern, C. W. *J. Am. Chem. Soc.* **1977**, *99*, 7042−7050.
(19) Zhao, Y.-L.; Wu, Y.-D. *J. Am. Chem. Soc.* **2002**, *124*, 1570−1571.
(20) Viswanathan, R.; Asensio, A.; Dannenberg, J. J. *J. Phys. Chem. A* **2004**, *108*, 9205−9212.
(21) Scheiner, S. *J. Phys. Chem. B* **2005**, *109*, 16132−16141.
(22) Chin, W.; Piuzzi, F.; Dimicoli, I.; Mons, M. *Phys. Chem. Chem. Phys.* **2006**, *8*, 1033−1048.
(23) Scheiner, S. *J. Phys. Chem. B* **2006**, *110*, 18670−18679.
(24) Scheiner, S. *J. Phys. Chem. B* **2007**, *111*, 11312−11317.
(25) Dixon, D. A.; Dobbs, K. D.; Valentini, J. J. *J. Phys. Chem.* **1994**, *98*, 13435−13439.
(26) Mannfors, B.; Mirkin, N. G.; Palmo, K.; Krimm, S. *J. Comput. Chem.* **2001**, *22*, 1933−1943.
(27) Frey, J. A.; Leutwyler, S. *J. Phys. Chem. A* **2006**, *110*, 12512−12518.
(28) Esrafili, M. D.; Behzadi, H.; Hadipour, N. L. *Theor. Chem. Acc.* **2008**, *121*, 135−146.
(29) Sun, C.-L.; Jiang, X.-N.; Wang, C.-S. *J. Comput. Chem.* **2009**, *30*, 2567−2575.
(30) Torii, H.; Tatsumi, T.; Kanazawa, T.; Tasumi, M. *J. Phys. Chem. B* **1998**, *102*, 309−314.
(31) Watson, T. M.; Hirst, J. D. *J. Phys. Chem. A* **2002**, *106*, 4858−7867.
(32) Langley, C. H.; Allinger, N. L. *J. Phys. Chem. A* **2003**, *107*, 5208−5216.
(33) Mirzaei, M.; Hadipour, N. L. *Struct. Chem.* **2008**, *19*, 225−232.
(34) Mathieu, S.; Trinquier, G. *Phys. Chem. Chem. Phys.* **2009**, *11*, 8183−8190.
(35) Colominas, C.; Luque, F. J.; Orozco, M. *J. Phys. Chem. A* **1999**, *102*, 6200−6208.
(36) Qian, W.; Mirkin, N. G.; Krimm, S. *Chem. Phys. Lett.* **1999**, *315*, 125−129.
(37) Vargas, R.; Garza, J.; Friesner, R. A.; Stern, H.; Hay, B. P.; Dixon, D. A. *J. Phys. Chem. A* **2001**, *105*, 4963−4968.
(38) Albrecht, M.; Rice, C. A.; Suhm, M. A. *J. Phys. Chem. A* **2008**, *112*, 7530−7542.
(39) Deshmukh, M. M.; Gadre, S. R. *J. Phys. Chem. A* **2009**, *113*, 7927−7932.
(40) Ham, S.; Cho, M. *J. Chem. Phys.* **2003**, *118*, 6915−6922.
(41) Vargas, R.; Garza, J.; Dixon, D. A.; Hay, B. P. *J. Am. Chem. Soc.* **2000**, *122*, 4750−4755.
(42) Frisch, M. J.; Trucks, G. W.; Schlegel, H. B.; Scuseria, G. E.; Robb, M. A.; Cheeseman, J. R.; Scalmani, G.; Barone, V.; Mennucci, B.; Petersson, G. A.; et al. *Gaussian 09*, revision B.01; Gaussian, Inc.: Wallingford, CT, 2009.
(43) Hyla-Kryspin, I.; Haufe, G.; Grimme, S. *Chem. Phys.* **2008**, *346*, 224−236.
(44) Pedzisa, L.; Hay, B. P. *J. Org. Chem.* **2009**, *74*, 2554−2560.
(45) Singh, P. C. *Chem. Phys. Lett.* **2011**, *515*, 206−209.
(46) Li, H.; Lu, Y.; Liu, Y.; Zhu, X.; Liu, H.; Zhu, W. *Phys. Chem. Chem. Phys.* **2012**, *14*, 9948−9955.
(47) Riley, K. E.; Murray, J. S.; Fanfrlík, J.; Rezác, J.; Solá, R. J.; Concha, M. C.; Ramos, F. M.; Politzer, P. *J. Mol. Model.* **2011**, *17*, 3309−3318.
(48) Hauchecorne, D.; Nagels, N.; Veken, B. J. v. d.; Herrebout, W. A. *Phys. Chem. Chem. Phys.* **2012**, *14*, 681−690.
(49) Lu, Y.; Liu, Y.; Li, H.; Zhu, X.; Liu, H.; Zhu, W. *J. Phys. Chem. A* **2012**, *116*, 2591−2597.
(50) Scheiner, S. *J. Phys. Chem. A* **2011**, *115*, 11202−11209.
(51) Zhao, Q.; Feng, D.; Sun, Y.; Hao, J.; Cai, Z. *Int. J. Quantum Chem.* **2011**, *111*, 3881−3887.
(52) Munusamy, E.; Sedlak, R.; Hobza, P. *ChemPhysChem* **2011**, *12*, 3253−3261.
(53) Boys, S. F.; Bernardi, F. *Mol. Phys.* **1970**, *19*, 553−566.
(54) Reed, A. E.; Weinhold, F.; Curtiss, L. A.; Pochatko, D. J. *J. Chem. Phys.* **1986**, *84*, 5687−5705.
(55) Reed, A. E.; Curtiss, L. A.; Weinhold, F. *Chem. Rev.* **1988**, *88*, 899−926.
(56) Moszynski, R.; Wormer, P. E. S.; Jeziorski, B.; van der Avoird, A. *J. Chem. Phys.* **1995**, *103*, 8058−8074.
(57) Werner, H.-J.; Knowles, P. J.; Manby, F. R.; Schütz, M.; Celani, P.; Knizia, G.; Korona, T.; Lindh, R.; Mitrushenkov, A.; Rauhut, G.; et al. *MOLPRO, Version 2006*; 2010.
(58) Gu, Y.; Kar, T.; Scheiner, S. *J. Mol. Struct.* **2000**, *552*, 17−31.
(59) Kryachko, E.; Scheiner, S. *J. Phys. Chem. A* **2004**, *108*, 2527−2535.
(60) Brenner, V.; Piuzzi, F.; Dimicoli, I.; Tardivel, B.; Mons, M. *J. Phys. Chem. A* **2007**, *111*, 7347−7354.

(61) Scheiner, S. *Int. J. Quantum Chem.* **2010**, *110*, 2775−2783.
(62) Scheiner, S. *J. Phys. Chem. B* **2009**, *113*, 10421−10427.
(63) Scheiner, S.; Kar, T. *J. Mol. Struct.* **2007**, *844*−*845*, 166−172.
(64) Tan, H.; Qu, W.; Chen, G.; Liu, R. *J. Phys. Chem. A* **2005**, *109*, 6303−6308.
(65) Kobko, N.; Dannenberg, J. J. *J. Phys. Chem. A* **2003**, *107*, 10389−10395.
(66) Wieczorek, R.; Dannenberg, J. J. *J. Am. Chem. Soc.* **2003**, *125*, 8124−8129.
(67) Ireta, J.; Neugebauer, J.; Scheffler, M.; Rojo, A.; Galvan, M. *J. Phys. Chem. B* **2003**, *107*, 1432−1437.
(68) Scheiner, S. *J. Mol. Struct.* **2010**, *976*, 49−55.
(69) Kar, T.; Scheiner, S. *Int. J. Quantum Chem.* **2006**, *106*, 843−851.
(70) Kar, T.; Scheiner, S. *J. Phys. Chem. A* **2004**, *108*, 9161−9168.